Terahertz Channel Performance in Emulated Falling Rain

Peian Li
Beijing Institute of Technology
Jianchen Wang
Beijing Institute of Technology
Liangbin Zhao
Beijing Institute of Technology
Jianjun Ma (jianjun_ma@bit.edu.cn)
Beijing Institute of Technology
Houjun Sun
Beijing Institute of Technology
Xiangyuan Bu
Beijing Institute of Technology
Jianping An
Beijing Institute of Technology

Research Article

Keywords: Terahertz wireless communication, falling rain, rain chamber, power attenuation, BER, raindrop size distribution

Posted Date: September 19th, 2022

DOI: https://doi.org/10.21203/rs.3.rs-744483/v2

Version of Record: A version of this preprint was published at Nano Communication Networks on December 9th, 2022. See the published version at https://doi.org/10.1016/j.nancom.2022.100431.

Abstract

The ever-increasing capacity demand (up to Tbps) in wireless connectivity is supposed can be satisfied by using terahertz frequency band ranging from 100 GHz to 10 THz. This has been proved over short channel distances in laboratory with high order modulation schemes (such as QPSK, QAM) employed. However, in outdoor adverse weathers, investigations on channel performance are not enough due to difficulties in outdoor measurements, and then more concentrations are still required. In this article, we report performance of terahertz channels in emulated falling rain in our lab by utilizing a broadband-pulsed terahertz channel and a 16-QAM modulated data stream. We observe that, the variability of raindrop size distribution is a major source of uncertainty in theoretical precipitation. We also find that the channel degradation in falling rain is mainly due to power attenuation, instead of phase dispersion which is negligible in our measurement.

1. Introduction

Wireless communication technology operating at terahertz (THz) frequency band provides a new solution for satisfying the demands on large data capacity and high physical layer security [1,2], which could not be achieved by existing radio frequency (RF) band and millimeter wave. For establishing 6G wireless networks, the THz band is regarded as a potential candidate in indoor and outdoor scenarios [3]. However, for outdoor applications, THz wireless channels suffer significant signal losses due to atmospheric weather effects, such as absorption and scattering [4]. Previously, amplitude attenuation and related channel performance degradation caused by water fog, dust cloud, rain and snow have been measured and investigated by employing an on-off keying (OOK) modulated THz links [5-7]. Higher order modulation schemes (such as QPSK, QAM etc.) are necessary to update the data rate with information on phase dispersion required, even though a theoretical investigation is provided in reference [8]. THz time-domain spectroscopy (THz-TDS) technique can be available for measuring and monitoring the variation of amplitude and phase and has been used to sense water vapor contained in air [9]. But there is lack of studies on their degradation in adverse outdoor weathers due to the difficulties for data recording, such as uncontrollable and unrepeatable weather conditions.

In this work, we investigate the influence of falling rain on THz channels by employing a commercial T-Ray 2000™ (Picometrix) THz-TDS system and a THz wireless setup with a 16-QAM modulation constellation scheme. A weather chamber was built in our laboratory to emulate stable and controllable falling rain. The lab condition can be reproducible and has been previously demonstrated [10,11]. We investigate and analyze the performance of a wireless terahertz channel in falling rain with a high order modulation scheme, which is usually difficult for actual outdoor measurements.

The rest of this article is organized as follows: Section 2 details the schematic diagram of the THz-TDS system with a data processing method mentioned. Section 3 shows measured data and comparison with theoretical calculation results. Section 4 presents experimental performance of a THz wireless channel in falling rain and finally Section 5 concludes this article.

2. Terahertz Tds Measurement

The schematic diagram of the measurement setup is shown in Fig. 1(a) with a commercial T-Ray 2000™ (Picometrix) terahertz time-domain spectrometer (TDS) employed. This is a conventional TDS system and has been employed in many publications [12-14]. THz pulses are generated by femtosecond optical pulses in the transmitter with a collimated beam diameter of 2 cm and then detected by subsequent optical pulses in the Ti:sapphire laser's pulse train. There are three gold plated mirrors (1, 2 and 3) used to reflect the THz radiation multiple times to extend the beam path inside the falling rain to be 4 m. When collecting the THz pulses to obtain the spectral attenuation, the system is set to a rapid scan mode with a 1000-pulse average calculation.

The whole rain chamber is composed of a rain generator (top part) for controllable rain generation and a beam path region for rain falling and signal propagation. The bottom plate of the rain generator is machined with 3261 holes in a cascade distribution. A kind of 31-gauge needle is sealed to each hole and could be epoxied to generate raindrops with an average diameter of 1.9 mm determined by the inner radius of the needle. The generator is filled with distilled water to emulate the actual material for rain, whose dielectric properties could be expressed by a double-debye model (D3M) [15]. The diameter of the needles is small enough such that when no air pressure is applied on the water inside the generator, no raindrops can be generated. The beam path region could communicate with the laboratory (air-conditioned by a central air-conditioning system) to maintain an identical temperature and humidity. For a channel inside this region, it can be regarded as propagating in free space.

The rainrate of the generated falling rain varies from 50 mm/hr to 500 mm/hr, and is linearly related to the air pressure inside the generator [10]. This means we could generate controllable and reproducible falling rain by controlling the air pressure. Fig. 1(b) shows that the raindrop size follows a log-normal distribution function as with a mean of logarithmic value μ = 0.674 and a standard deviation of logarithmic value σ = 0.157. The parameter D represents the diameter of raindrop particles, which is independent of the pressure and rainrate. It is always true that the rain droplets we generated are spherical. Parameter N_{Rr} refers to the total number of raindrop particles in a unit volume [16], which depends on the pressure and rainrate.

Inverse fast Fourier transformation is conducted on the measured data, the amplitude spectra of the pulses passing free space (no rain generated) and falling rain are shown in Fig. 1(c) with a rainrate (*Rr*) of 256 mm/hr. Strong water vapor absorption lines at 0.56 THz, 0.75 THz and 0.98 THz are clearly observable for both curves. Phase spectra is also obtained as shown in Fig. 1(d) without any unwrapping algorithms used. Obvious jumps, corresponding to the strong absorption lines of water vapor [17], are observable for both curves. The phase shift due to falling rain, which could be obtained by comparing both phase spectra curves, is negligible in this work, except at frequencies corresponding to water absorption lines.

3. Experimental Data And Theoretical Modeling

Mie scattering theory [18] can be used to calculate the signal loss due to absorption and scattering caused by raindrop particles, because the size of the raindrop particles we generated is in the scale of millimeter [19], which is usually comparable to or larger than the THz wavelength. For very small particles, solution given by the Mie theory approaches the Rayleigh approximation [20]. This method systematically describes the scattering mechanism of THz waves by particles of various sizes in the atmosphere. A commonly used theoretical model provided by the ITU Recommendation Sector (ITU-R) [21,22] for gaseous absorption based on the physical model MPM93[23]. ITU-R also provides a prediction model for rain attenuation by equation with the values of a and k determined for a given frequency in the range of 1 GHz to 1 THz, which was given by fitting measurement data.

Raindrop size distribution can be affected by various microphysical and dynamic processes inside and below cloud layers. In practical applications, empirical mathematical formulas derived from observed size spectra have been used to approximate natural snow size distributions. Raindrops usually follow exponential [24, 25], Gamma [26] and log-normal distribution [27] in present published investigations. Marshall-Palmer (M-P) distribution [24] is a typical kind of exponential function, and can be proposed for both raindrop and snow description [28]. It is expressed as $N(r) = N_0 \exp(-\Lambda r)$, where, N is the number of rain droplet radius of $r + dr$ in unit volume. Parameter r is the radius of rain droplet. Parameter $N_0 = 16\times10^3$ [$m^{-3}\cdot mm^{-1}$] and $\Lambda = 8.2Rr^{-0.21}$ [mm^{-1}] are two characteristic parameters and can be retrieved rainrate Rr in mm/hr [29].

The calculation results are shown in Fig. 2 with measured data at 140, 220, 340 and 675 GHz. These frequencies lie in the transparency window and has been used for wireless link setup in several publications [2]. The gaseous absorption, especially due to water vapor under a relative humidity of 37%, is included in the model. An obvious discrepancy between the measurements and the calculated result by ITU-R model or Mie scattering theory with M-P distribution. However, the calculation by Mie scattering together with the log-normal distribution is much better agreed with the measured data. This means Mie scattering is a good theory for the precipitation of signal losses due to falling rain, when a correct raindrop size distribution is ready [30].

4. Terahertz Data Link Measurement

To see the influence of the falling rain on higher order constellation modulation schemes, a 16-QAM THz wireless communication setup is built with its schematic diagram shown in Fig. 3(a). A Xilinx Vertix-7 serial FPGA (XC7VX485T) is used to generate a 16-QAM modulated signal at an intermediate frequency (IF) of 1.25GHz with a data rate of 5 Gbps. The generated digital sequence from FPGA is converted into an analog signal by a DAC (MD662H). After that, it is mixed with a radio frequency (RF) of 162 GHz by a subharmonic mixer (110-170GHz) which is driven by an 81GHz reference signal from an ×6 multiplier. Then, the signal is launched out by a THz antenna. On the receiver side, a low noise amplifier amplifies the D-band signal captured by another identical THz antenna and sends its output to a subharmonic mixer to obtain the IF signal which can be converted to digital sequence by an ADC (EV10AQ190). A Xilinx XC7VX690T FPGA is used for synchronization processing and demodulation operation. The output

binary sequence would be compared with the transmitting binary sequence, and then the Eb/N0 parameter can be derived by calculating the bit-error-ratio (BER) easily.

When the 162 GHz channel propagates through the falling rain with a rainrate of 350 mm/hr, variation of BER value with respect to transmitted THz power is recorded and shown in Fig. 4(b). After through the falling rain, the BER values at the received power below -40.3 dBm could not be recorded due to the scattering and absorption by falling rain droplets. An obvious BER degradation caused by falling rain can be observed when compared with that in free space under the same transmitted power. However, the slopes of both curves are almost identical, which means the BER degradation is mainly due to the power loss by falling rain. In other words, the phase of the channel is more resilience to the influence by falling rain than the amplitude.

When we mount the receiver on a movable rail which permits it to translate along an axis perpendicular to the incoming beam's propagation direction as in Fig. 3(a). By scanning the detector along this line, we map the spatial distribution of the beam arriving at the receiver side. A power loss of 0.5 dB (from -36.4 dBm to -36.9 dBm) due to rain is observed in Fig. 4(a) along the beam axis (receiver position of 0 m), which is consistent with our prediction in Fig. 2 for a channel distance of 1 m. The corresponding BER degradation is shown in Fig. 4(b), which changes from 7.6×10^{-11} in free space to 6.5×10^{-10} in falling rain. An error rate of 10^{-10} could not be achieved in falling rain due to the signal loss. It should be noted that there is no obvious fluctuation observed in both the power and BER evolution curves, which confirms that the falling rain has negligible influence on the phase of the signal instead of its amplitude.

5. Conclusion

In this article, we conduct a study on performance of terahertz wireless channels in emulated falling rain by using a commercial THz time-domain spectroscopy system and a 16-QAM modulated THz wireless channel. The Mie scattering theory is confirmed to be a correct method to predict the attenuation when an accurate raindrop size distribution is chosen or measured. The phase of the wireless channel is more resistive to the falling rain than the amplitude. Further efforts will be conducted to include the influence of rain-lines and wind-induced pole vibration [8], which should be considered in actual outdoor scenarios.

References

[1] J. Ma et al., "Security and eavesdropping in terahertz wireless links," Nature, vol. 563, p. 89, Oct 15 2018, doi: 10.1038/s41586-018-0609-x.

[2] T. Nagatsuma, G. Ducournau, and C. C. Renaud, "Advances in terahertz communications accelerated by photonics," Nature Photonics, vol. 10, no. 6, pp. 371-379, 2016, doi: 10.1038/nphoton.2016.65.

[3] M. H. Alsharif, A. H. Kelechi, M. A. Albreem, S. A. Chaudhry, M. S. Zia, and S. Kim, "Sixth Generation (6G) Wireless Networks: Vision, Research Activities, Challenges and Potential Solutions," Symmetry, vol. 12, no. 4, p. 676, 2020, doi: 10.3390/sym12040676.

[4] Z. Lai et al., "Impact of Meteorological Attenuation on Channel Characterization at 300 GHz," Electronics, vol. 9, no. 7, p. 1115, 2020.

[5] A. Hirata et al., "Effect of Rain Attenuation for a 10-Gb/s 120-GHz-Band Millimeter-Wave Wireless Link," IEEE Transactions on Microwave Theory and Techniques, vol. 57, no. 12, pp. 3099-3105, 2009, doi: 10.1109/tmtt.2009.2034342.

[6] J. F. Federici, J. Ma, and L. Moeller, "Review of weather impact on outdoor terahertz wireless communication links," Nano Communication Networks, vol. 10, pp. 13-26, 2016, doi: 10.1016/j.nancom.2016.07.006.

[7] J. Ma, J. Adelberg, R. Shrestha, L. Moeller, and D. M. Mittleman, "The Effect of Snow on a Terahertz Wireless Data Link," Journal of Infrared, Millimeter and Terahertz Waves, vol. 39, no. 6, pp. 505-508, 2018, doi: 10.1007/s10762-018-0486-2.

[8] "Millimeter-Wave and Terahertz Fixed Wireless Link Budget Evaluation for Extreme Weather Conditions."

[9] M. Mandehgar, Y. Yang, and D. Grischkowsky, "Atmosphere characterization for simulation of the two optimal wireless terahertz digital communication links," Optics Letters, vol. 38, no. 17, pp. 3437-40, Sep 01 2013, doi: 10.1364/OL.38.003437.

[10] J. Ma, F. Vorrius, L. Lamb, L. Moeller, and J. F. Federici, "Comparison of Experimental and Theoretical Determined Terahertz Attenuation in Controlled Rain," (in English), Journal of Infrared, Millimeter and Terahertz Waves, vol. 36, no. 12, pp. 1195-1202, Dec 2015, doi: 10.1007/s10762-015-0200-6.

[11] J. Ma, F. Vorrius, L. Lamb, L. Moeller, and J. F. Federici, "Experimental Comparison of Terahertz and Infrared Signaling in Laboratory-Controlled Rain," (in English), Journal of Infrared, Millimeter and Terahertz Waves, vol. 36, no. 9, pp. 856-865, Sep 2015, doi: 10.1007/s10762-015-0183-3.

[12] B. Ferguson and X.-C. Zhang, "Materials for Terahertz Science and Technology," Nat Mater, vol. 1, no. 1, pp. 26-33, 2002, doi: 10.1038/nmat708.

[13] D. A. Zimdars, "Fiber-pigtailed terahertz time domain spectroscopy instrumentation for package inspection and security imaging," presented at the Terahertz for Military and Security Applications, Orlando, Florida, United States, 2003.

[14] Z. Hossain, S. H. Vedant, C. R. Nicoletti, and J. F. Federici, "Multi-user Interference Modeling and Experimental Characterization for Pulse-based Terahertz Communication," pp. 1-6, 2016, doi: 10.1145/2967446.2967462.

[15] F. T. Ulaby and D. G. Long, Microwave Radar and Radiometric Remote Sensing. Ann Arbor, Michigan: University of Michigan Press, 2013.

[16] S. Ishii, S. Sayama, and T. Kamei, "Measurement of Rain Attenuation in Terahertz Wave Range," Wireless Engineering and Technology, vol. 02, no. 03, pp. 119-124, 2011, doi: 10.4236/wet.2011.23017.

[17] C. Jördens, S. Wietzke, M. Scheller, and M. Koch, "Investigation of the water absorption in polyamide and wood plastic composite by terahertz time-domain spectroscopy," Polym Test, vol. 29, no. 2, pp. 209-215, 2010, doi: 10.1016/j.polymertesting.2009.11.003.

[18] D. J. Lockwood, "Rayleigh and Mie Scattering," in Encyclopedia of Color Science and Technology, M. R. Luo Ed. New York, NY: Springer, 2016.

[19] H. R. Pruppacher and J. D. Klett, Microphysics of clouds and precipitation. Dordrecht: Kluwer Academic Publishers, 1997.

[20] D. Deirmendjian, Electromagnetic scattering on spherical polydispersions. New York: American Elsevier Publishing, 1969.

[21] "Recommendation ITU-R P.676-11: Attenuation by Atmospheric Gases." https://www.itu.int/dms_pubrec/itu-r/rec/p/R-REC-P.676-11-201609-I!!PDF-E.pdf (accessed.

[22] " International Telecommunication Union Recommendation (ITU-R) P.676-12: Attenuation by atmospheric gases and related effects." https://www.itu.int/rec/R-REC-P.676-12-201908-I (accessed.

[23] H. Liebe, G. Hufford, and M. Cotton, "Propagation modeling of moist air and suspended water/ice particles at frequencies below 1000 GHz," presented at the Proceedings of AGARD, 52nd Specialists Meeting of the Electromagnetic Wave Propagation Panel, 1993.

[24] J. S. Marshall and W. M. Palmer, "The distribution of raindrops with size," Journal of Meteorology, vol. 5, no. 4, pp. 165-166, 1948.

[25] G. Zhang, M. Xue, Q. Cao, and D. Dawson, "Diagnosing the Intercept Parameter for Exponential Raindrop Size Distribution Based on Video Disdrometer Observations: Model Development," Journal of Applied Meteorology and Climatology, vol. 47, no. 11, pp. 2983-2992, 2008.

[26] D. A. de Wolf, "On the Laws-Parsons distribution of raindrop sizes," Radio Science, vol. 36, pp. 639-642, 2001.

[27] C. Cerro and B. Codina, "Modeling raindrop size distribution and Z(R) relations in the Western Mediterranean Area," Journal of Applied Meteorology, vol. 36, no. 11, pp. 1470-1479, 1997.

[28] R. E. Passarelli, "Theoretical and Observational Study of Snow-Size Spectra and Snowflake Aggregation Efficiencies," Journal of the Atmospheric Sciences,, vol. 35, no. 5, pp. 882-889, 1978.

[29] Y. Amarasinghe, W. Zhang, R. Zhang, D. M. Mittleman, and J. Ma, "Scattering of Terahertz Waves by Snow," Journal of Infrared, Millimeter, and Terahertz Waves, vol. 41, pp. 215-224, 2019.

[30] M. Yoseva, H. Hashiguchi, M. Vonnisa, L. Luini, S. Nugroho, and M. A. Shafii., "Characteristics of Rain Attenuation for Microwave-to-terahertz Waveband from Raindrop Size Distribution Observation in Indonesia," presented at the PhotonIcs & Electromagnetics Research Symposium - Spring (PIERS-Spring), Rome, Italy, 2019.

Figures

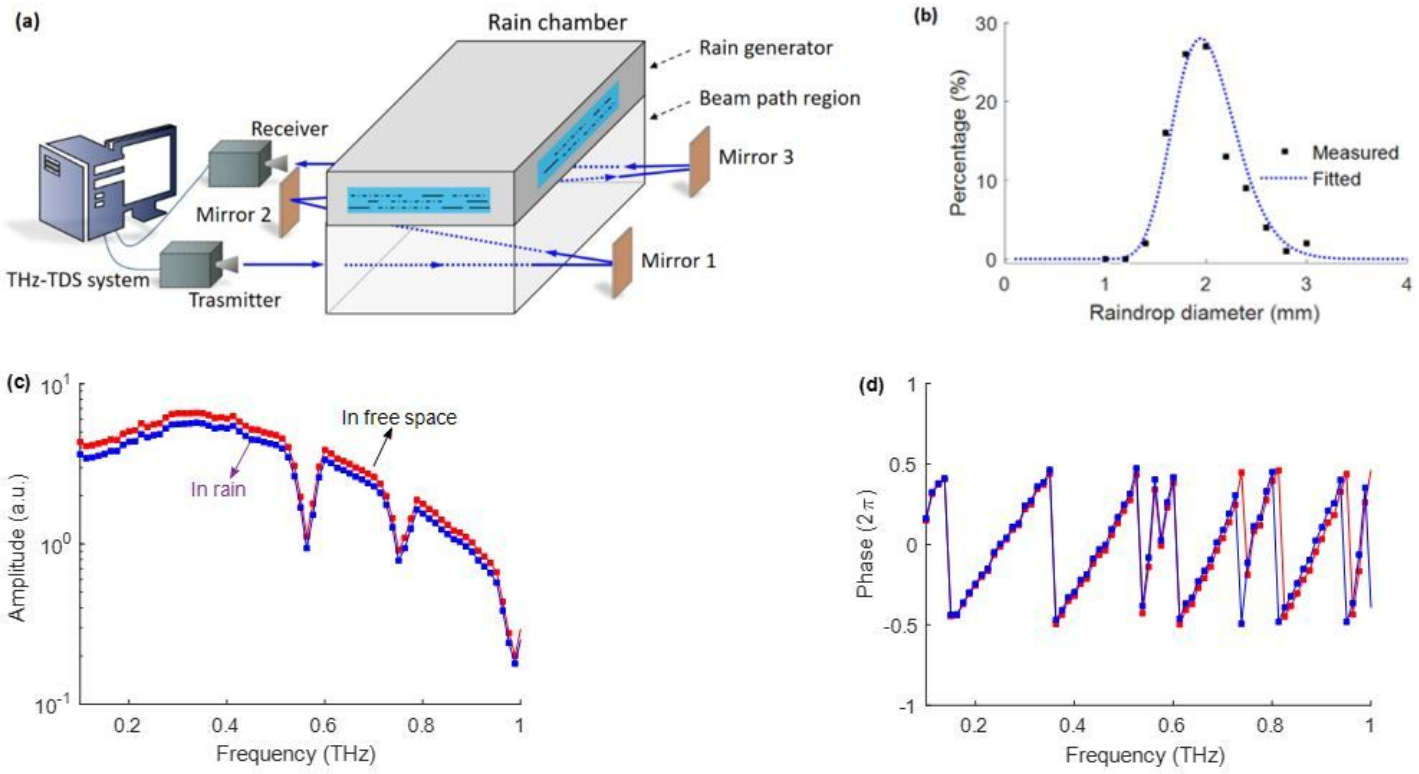

Figure 1

(a) Schematic measurement setup. The rain generator has a dimension of 1.0×0.2×0.2 m3 in L×W×H. It is constructed from aluminum with a transparent Plexiglas window in the center of the side panel in order to monitor the water level while the system is running. The beam path region has a dimension of 1.0×0.2×0.5 m3 in L×W×H. Mirrors (1, 2 and 3) are gold plated and could be used to extend the beam path inside the chamber to be 4 m. (b) Rain drop size distribution. A log-normal distribution fit to measured data is shown with a mean of logarithmic value μ= 0.674 and a standard deviation of logarithmic value σ = 0.157. The measured data was obtained from reference [10]. (c) The broadband-pulsed terahertz source is used to launch a THz pulse into free space and falling rain. The red curve stands for the received signal propagates in free space and the blue one for the signal passing falling rain with a rainrate of 256 mm/hr. (d) Phase performance of THz channels due to falling rain with the same legend as Fig. 1(c). There is no unwrapping algorithms used.

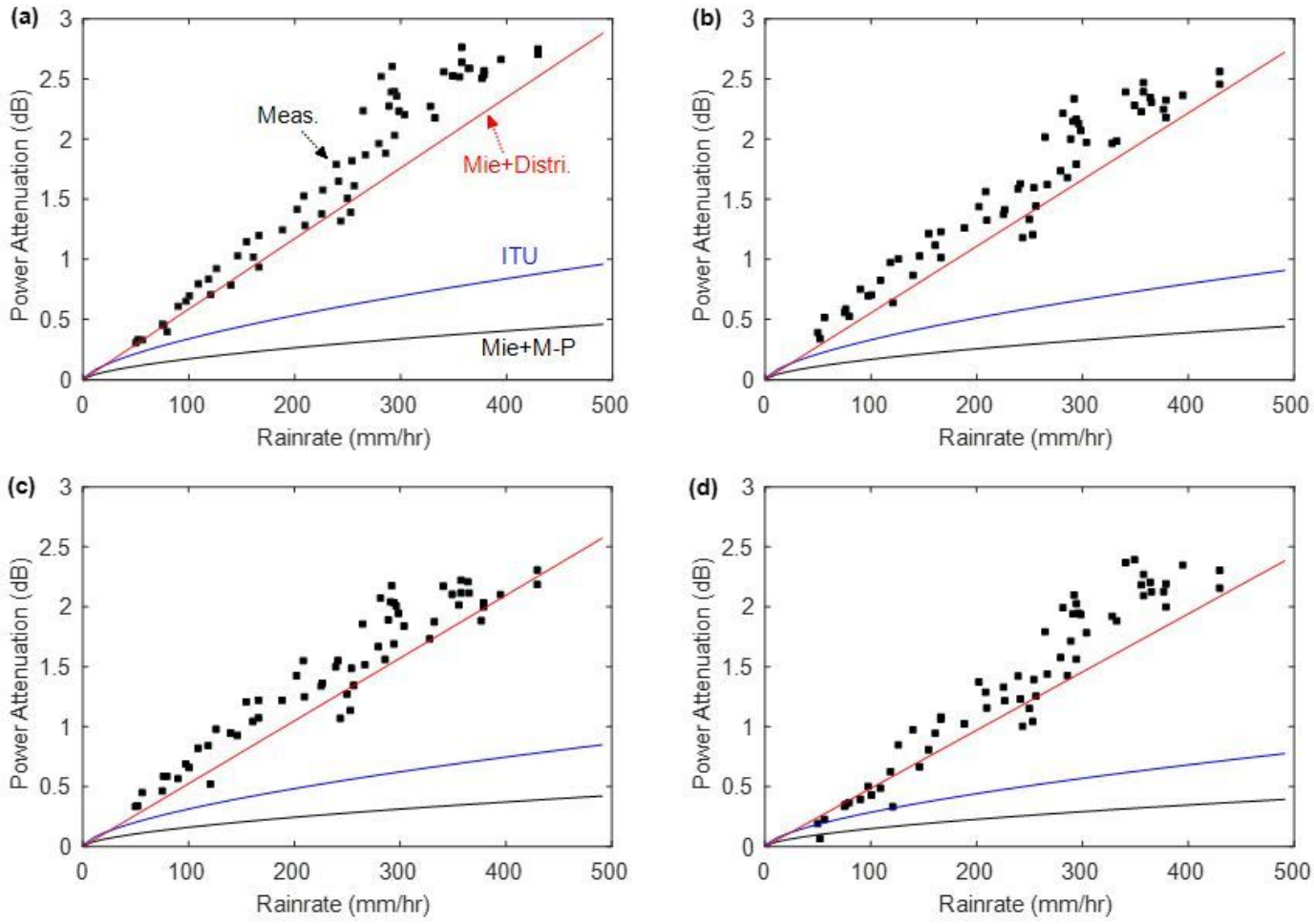

Figure 2

Power attenuation on wireless channels operating at (a) 140 GHz, (b) 220 GHz, (c) 340 GHz and (d) 675 GHz caused by falling rain with rainrate changing from 50 mm/hr to 450 mm/hr. The black squares represent measured data obtained from the difference between the amplitude spectra in free space and in falling rain. The solid curves stand for calculated results. The red one is for calculation by using Mie scattering theory and the log-normal distribution of raindrop size as in Fig. 1(b). The blue one is for ITU-R model. The black one is by the Mie scattering theory and the Mashall-Palmer (M-P) distribution of raindrop size.

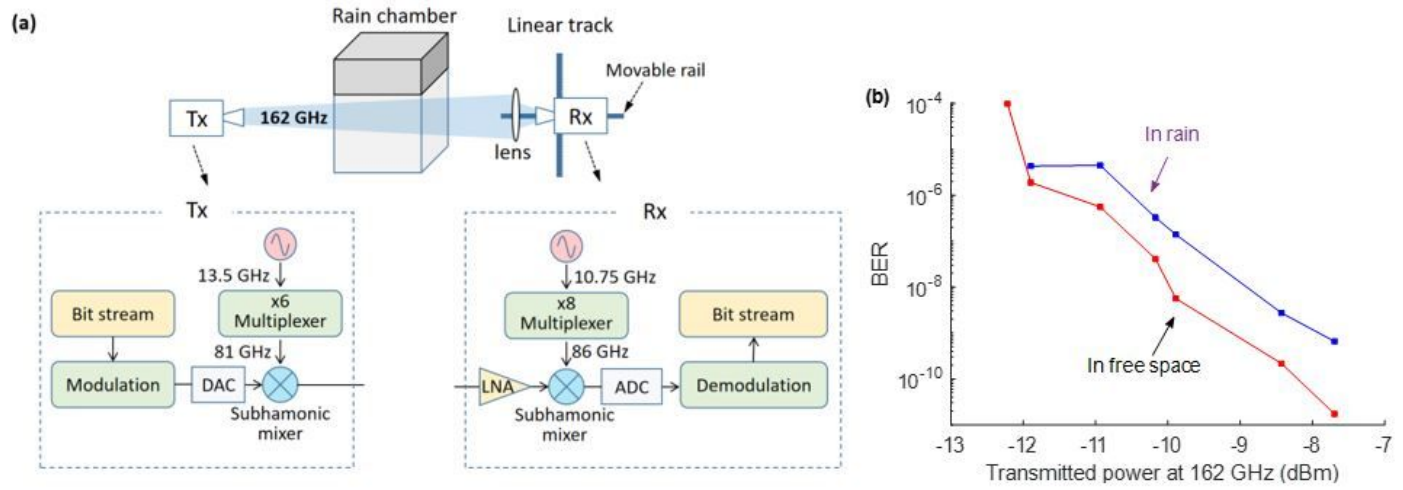

Figure 3

Schematic diagram and degradation of a modulated THz channel as a function of transmitted power. (a) Schematic measurement setup, with one transmitter at 162 GHz, and with the receiver mounted on a linear rail to vary the position of the receiver. (b) Measured real-time BER performance of the THz link as a function of the transmitted power at a data rate of 5 Gbps. Values are recorded both after propagating through free space (red) and falling rain (blue) with the receiver fixed along the beam axis.

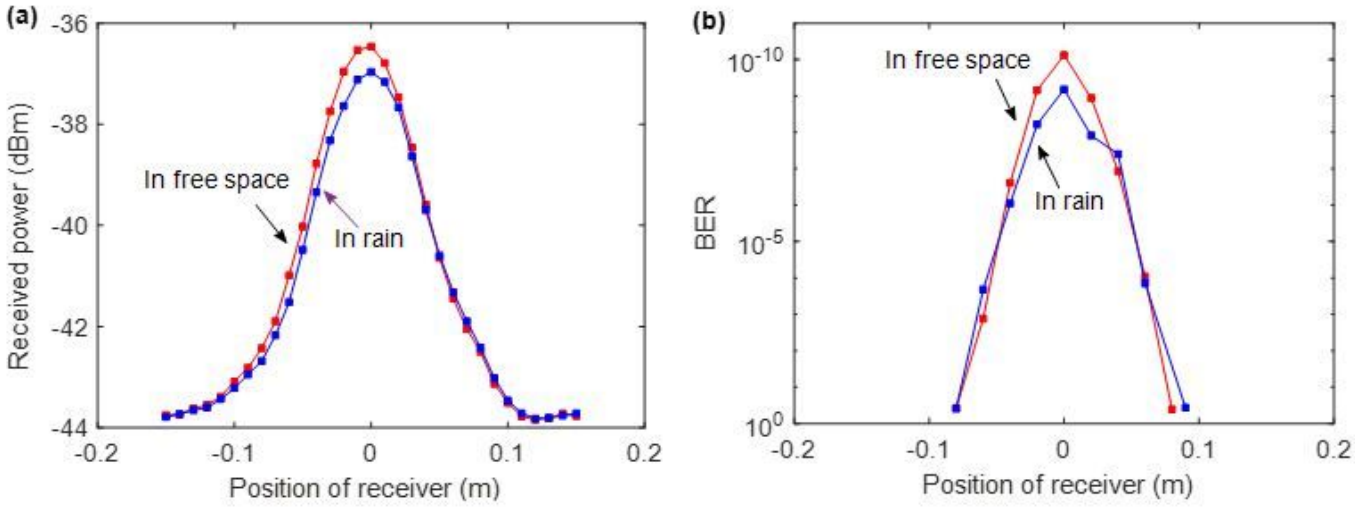

Figure 4

Power and BER patterns of the THz channel in falling rain. (a) Power pattern measured when channel propagates through free space (red) at temperature T =17°C, humidity RH 34% and falling rain (blue) at rainrate Rr = 350 mm/hr, temperature T=17°C, humidity RH 34%. (b) Measured BER evolution corresponding to the power patterns in Fig. 4(a).